

February 2003

Orientation of self-assembled block copolymer cylinders perpendicular to electric field in mesoscale film

S. Elhadj
Virginia Tech, Blacksburg, Virginia

J. W. Woody
Virginia Tech, Blacksburg, Virginia

V. S. Niu
Virginia Tech, Blacksburg, Virginia

Ravi Saraf
University of Nebraska-Lincoln, rsaraf2@unl.edu

Follow this and additional works at: <http://digitalcommons.unl.edu/cbmesaraf>

 Part of the [Biomechanics and Biotransport Commons](#)

Elhadj, S.; Woody, J. W.; Niu, V. S.; and Saraf, Ravi, "Orientation of self-assembled block copolymer cylinders perpendicular to electric field in mesoscale film" (2003). *Ravi Saraf Publications*. 4.
<http://digitalcommons.unl.edu/cbmesaraf/4>

This Article is brought to you for free and open access by the Chemical and Biomolecular Research Papers -- Faculty Authors Series at DigitalCommons@University of Nebraska - Lincoln. It has been accepted for inclusion in Ravi Saraf Publications by an authorized administrator of DigitalCommons@University of Nebraska - Lincoln.

Orientation of self-assembled block copolymer cylinders perpendicular to electric field in mesoscale film

S. Elhadj, J. W. Woody, V. S. Niu, and R. F. Saraf^{a)}

Department of Chemical Engineering, Virginia Tech, Blacksburg, Virginia 24061

(Received 9 October 2002; accepted 11 December 2002)

The possibility of using self-assembled films of block polymers as templates to fabricate nanoscale structures for devices has attracted great attention towards this class of material. Self-assembly of a block copolymer can be directed by using an electric field to orient features (i.e., ~ 10 -nm-diam cylinders) *parallel* to the electric field, making the material more attractive as a nanoscale lithography mask. In this letter we describe an approach to influence the electric field orientation phenomena by interfacial effects. As a result, the 15-nm-diam polystyrene cylinders of the polystyrene–polyisoprene–polystyrene triblock copolymer orient *perpendicular* to the electric field. The described approach along with the previous method can produce a directed self-assembly to fabricate complex nanoscale structures with orthogonally oriented nanoscale width lines. © 2003 American Institute of Physics. [DOI: 10.1063/1.1543253]

Self-assembly¹ is emerging as a powerful principle to fabricate organized structures and devices in the mesoscale, bridging the gap between molecular and macroscopic scales.² Monolayers of block copolymers³ are attractive template materials that self-assemble to create a broad range of nanostructures. Typically, the minority component can be tailored to spontaneously order on a periodic lattice to form a variety of features, such as spheres, cylinders, etc., with a characteristic length on the order of 10^1 nm.⁴ The ordered structure, composed of chemically dissimilar discrete features and of a continuous matrix, may be selectively etched away to form templates by a variety of wet and dry processing methods.^{5–8} Furthermore, these nanoscale discrete features may be manipulated by electric field,⁹ mechanical strain,¹⁰ rapid solvent evaporation,¹¹ or by chemically tailoring the film/substrate interface¹² to create an anisotropic ordered structure.

Several interesting functional structures and devices have been demonstrated using block copolymer templates. For example, GaAs/GaAs quantum dots for laser emission,¹³ array on nanowires,¹⁴ and nanoscale patterned barium titanate.¹⁵ In the above manipulation techniques,^{9–11} the orientation of the anisotropic feature, viz., the axis of the cylinder, orients *parallel* to the external electric field, mechanical deformation, or the solvent (diffusion) flow direction. In this study we describe a method to induce the orientation of cylinders *perpendicular* to the electric field. A combination of the method discussed, with the prior electric field orientation techniques⁹ may hopefully lead to a highly versatile approach to fabricate long-range complex patterns of nanoscale width lines.

Orientation of an anisotropic dielectric body in a dielectric media due to external electric field, \mathbf{E}_O , occurs due to a depolarization field, \mathbf{E}_P , which is normal to the interface between two dielectric materials. The system minimizes its free energy by orienting the dielectric body such that the torque at the interface $\chi(\mathbf{E}_P + \mathbf{E}_O) \times \mathbf{E}_O$ is zero, with χ rep-

resenting the dielectric susceptibility.¹⁶ In ordered block copolymer film with cylindrical discrete components there are two free energy (per unit volume) minima: F_{\parallel} and F_{\perp} , corresponding to parallel and perpendicular orientations, respectively.^{16,17} The difference is given by^{17,18}

$$\Delta F_e = F_{\parallel} - F_{\perp} = -E_O^2 \epsilon_O \frac{(\epsilon_{PI} - \epsilon_{PS})^2}{2(\epsilon_{PI} + \epsilon_{PS})}, \quad (1)$$

where ϵ_O is the permittivity in vacuum and where ϵ_{PI} and ϵ_{PS} are the dielectric constants of polyisoprene (PI) and polystyrene (PS), respectively. The $\Delta F_e < 0$ indicates that the free-energy well for alignment parallel to the electric field is deeper than the transverse orientation. In this study we describe a method to trap the orientation in the shallower energy well corresponding to orientation perpendicular to the electric field.

Films of a polystyrene–polyisoprene–polystyrene [semiconductor–insulator–semiconductor (SIS)] triblock copolymer were prepared by spin casting from a 0.95% (*w/v*) toluene solution on a SiO₂/Si wafer with Au electrodes. The molecular weights of polystyrene and polyisoprene blocks are 18 000 and 64 000 g/mol, respectively, with polydispersity of < 1.09 . The thermally grown SiO₂ layer is ~ 500 nm thick. The Au electrodes (20 μ m apart) and Cr adhesion layers are 200 and 20 nm thick, respectively. Prior to polymer deposition, the wafer is immersed overnight in ethanol followed by a 30 min at 110 °C in N₂ atmosphere. The spin-cast film is immediately placed in a sealed chamber (~ 160 cm³) for 24 h at 22 °C under an electric field ranging from 0 to 150 kV/cm.

As the solvent evaporates the film commences to order with discrete cylindrical component of PS in the PI matrix. In order to achieve better long-range order, the rate of evaporation is reduced by adding a reservoir of solvent (75 μ l) in the chamber, similar to the solvent-annealing process described before for an identical polymer system.¹⁹ Atomic force microscope (AFM) was used to study the surface morphology in tapping mode. A film thickness of 19.5 ± 2.8 nm was obtained on films with dry spots. Since the diameter of

^{a)}Author to whom correspondence should be addressed; electronic mail: rsaraf@vt.edu

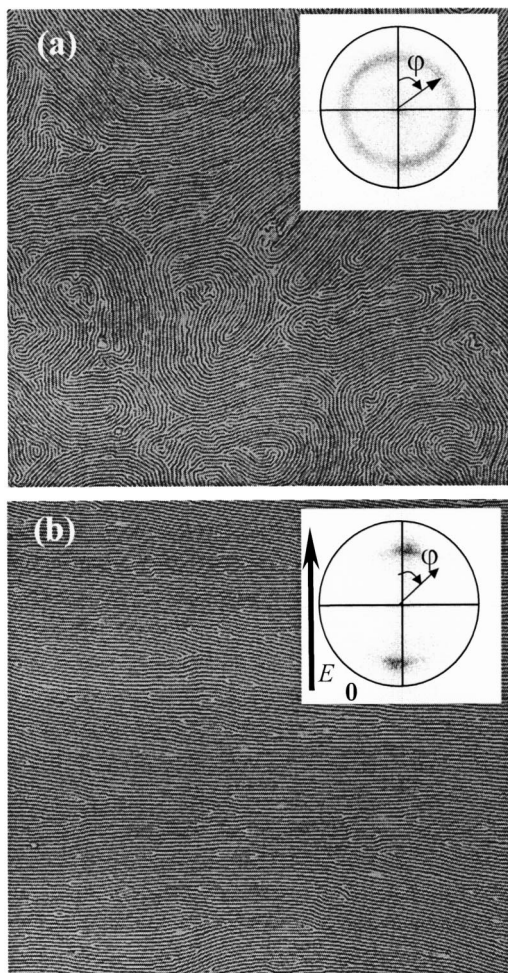


FIG. 1. AFM phase images of the SIS block copolymer at E_0 of (a) 0 and (b) 125 kV/cm. The height of the lighter, PS cylinders is 2.06 ± 0.55 nm, and the pitch is 34 ± 3.2 nm. The FFT image in the inset shows the first-order peak (i.e., FFT amplitude maxima) corresponding to the pitch. The distribution of the FFT amplitude along the azimuthal angle, ϕ indicates that the cylinders are oriented *perpendicular* to the electric field. A slight distribution at $E_0=0$ is observed due to limited sample size of $25 \mu\text{m}^2$. In both cases the image is obtained from the central region between the electrodes.

the PS cylinders measured by transmission electron microscopy is ~ 15 nm,¹⁹ the ordered structure is a two-dimensional (2D) array of PS cylinders in the PI matrix.

Figures 1(a) and 1(b) compare 5 by 5 μm AFM phase images of the surface morphology of the block copolymer between the electrodes at $E_0=0$ and $E_0=125$ kV/cm, respectively. Lighter regions are PS cylinders while darker regions are the PI matrix. The images show that the cylinders are highly oriented when ordered under an electric field in contrast to $E_0=0$. The corresponding fast-Fourier-transform (FFT) pattern of the two images shown in the insets of Figs. 1(a) and 1(b) have a “halo” corresponding to intercylinder packing. The intensity of the halo is nominally uniform along the azimuthal angle, ϕ , for $E_0=0$ [Fig. 1(a)], indicating that the orientation is random. A slight nonuniform distribution occurs because the sample size of 5 by 5 μm is not large enough compared to the $\sim 1 \mu\text{m}$ grains seen in the AFM image. In contrast, the FFT of the AFM image corresponding to $E_0=125$ kV/cm [Fig. 1(b)] shows a sharp azimuthal distribution. The peak of the intercylinder halo at $\phi=0$ indicates that the cylinders are along the $\phi=0$ and π , consistent with the AFM image.

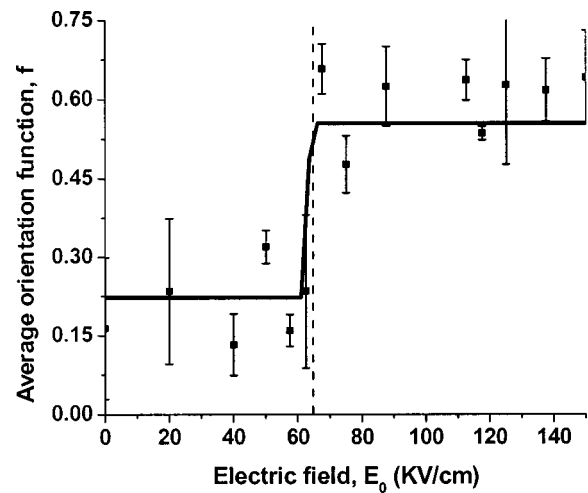


FIG. 2. Average orientation (f) defined in Eq. (2) as a function of applied electric field indicates a threshold field, E_{th} at 65 ± 5 kV/cm (shown as the dashed line). The nominal orientation of $f \sim 0.15$ at low voltages indicates that the “grain size” of the PS cylinder domains is comparable to the image size. Error bars are calculated from three 5 by 5 μm images for each sample.

The normalized magnitude of the FFT amplitude maxima along the azimuthal axis is the orientation distribution of the cylinders. Thus, the average orientation angle, $\langle \cos^2 \phi \rangle$, is given by

$$\langle \cos^2 \phi \rangle = \frac{\int_{-\pi/2}^{\pi/2} \cos^2 \phi I(\phi) d\phi}{\int_{-\pi/2}^{\pi/2} I(\phi) d\phi}, \quad (2)$$

where $I(\phi)$ is the FFT amplitude at the maxima of the halo. Since the cylinders form a 2D monolayer, the average orientation is defined as $f = \langle 2 \cos^2 \phi - 1 \rangle$. From Eq. (2), for random orientation, $I(\phi) = \text{constant}$ leads to $f=0$ and for perfect orientation $I(\phi) = \delta(\phi)$ leads to $f=1$ [$\delta(\phi)$ is the Dirac delta function]. Figure 2 shows f as a function of E_0 . The solid curve is a fitted S-shape function that indicates a threshold field E_{th} in the range of 60–70 kV/cm to influence alignment of the cylinders perpendicular to the electric field. For $E_0 < E_{th}$, f is low, indicating no orientation. A finite value f below 0.15 for low fields is due to small sample size of the 5 by 5 μm area. Because of long-range order in these films, the $25 \mu\text{m}^2$ area at $E_0=0$ always exhibits $f > 0$. A high orientation close to $f \sim 0.7$ is obtained for field above E_{th} . The saturation at low value of $f \sim 0.73$ is due to disorientations caused by dislocation and disclination defects on the 5 by 5 μm sample. Thus, due to the statistical limitations from the limited small sample size, the threshold may not be apparent unless a nonlinear fitting analysis is performed. In addition, there is a statistically significant difference ($p < 0.0001$) between the f value (i.e., orientation) under high ($E_0 > E_{th}$) versus low ($E_0 < E_{th}$) fields.

Similar low saturation f values are observed for electric field orientation where cylinders align parallel to the in-plane field.⁹ However, for alignment parallel to the electric field that is perpendicular to the film thickness, $f \sim 0.9$ is observed by the small-angle x-ray scattering (SAXS) technique.¹⁸ A large value may partly be explained by the $> 10^4$ times larger sample area for SAXS compared to the AFM method. The orientation behavior in Fig. 2, similar to parallel alignment,^{9,18} exhibits a switching field of E_{th} such that the orientation above and below E_{th} is nominally independent of the E field. Similar to the Freederickz transition in liquid

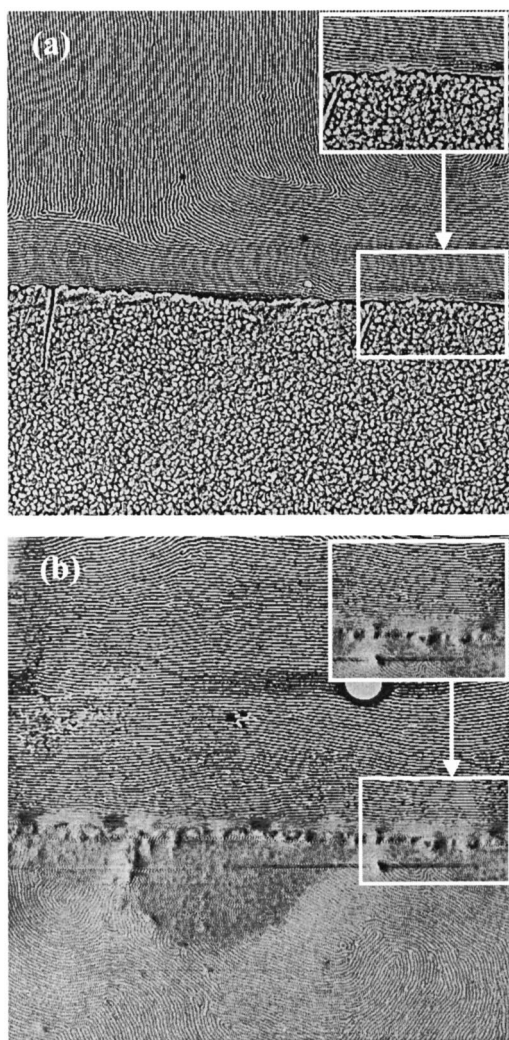


FIG. 3. AFM phase images of the SIS block copolymer at E_O of (a) 0 and (b) 125 kV/cm, taken at the edge of the Au electrodes (the bottom half plane of the image). A preferential ordering of the PS cylinders parallel to the Au electrode edge is apparent in both cases. However, the orientation is significantly extended over a longer range in the presence of an electric field. The inset is a $2\times$ magnification.

crystals,²⁰ the threshold effect is explained as extra (enthalpic) energy required to overcome the film/substrate interaction.¹⁸

The perpendicular orientation of the cylinders with respect to the electric field is qualitatively explained as follows. PS has ~ 6 dyn/cm higher surface energy than PI, causing the latter component of the block copolymer to segregate at the polymer/Au and polymer/Si interfaces.²¹ The preferential wetting of PI over PS at the Au interface will influence the PS cylinders to orient along the Au edge. Orientation of cylinders along the edge is similar to graphoepitaxy observed for block copolymers in 1–10 μm SiO_2 trenches.²² As the ordering process continues due to gradual solvent evaporation, the alignment of PS cylinders will nucleate at the edge and propagate into the film. Figure 3(a) shows such spontaneous alignment of PS cylinders along the edge under no electric field. The alignment propagates well above 500 nm (~ 16 – 30 cylinders) from the edge. On application of an electric field perpendicular to the edge, this alignment process should be further enhanced due to the second (but shallower) free-energy minima where the cylinders are *perpen-*

dicular to the electric field. Figure 3(b) shows the orientation propagates well over 2500 nm (i.e., >80 cylinders) when the film is ordered under electric field. Thus, due to a second force field caused by interfacial effects, the system is trapped into the shallower minima where the cylinders orient perpendicular to the electric field.

If the ordering process was by “homogeneous nucleation,” the total free energy will be a combination of $\Delta F_e \sim -E_O^2 < 0$ [see Eq. (1)] and $\Delta F_\sigma = F_{\parallel} - F_{\perp} > 0$ (since orientation parallel to electrode edge is favored). Thus, at some threshold electric field, the total free energy, $\Delta F_\sigma + \Delta F_e = 0$, i.e., the two effects will balance out. Beyond this threshold field the orientation should be *parallel* to the electric field. Since no *parallel* alignment of the cylinders was detected up to $E_O = 150$ kV/cm for these thin films composed of monolayers of PS cylinders, the suggested mechanism of “heterogeneous nucleation” initiated at the electrode edge may be a likely mechanism.

One of the authors (R.F.S.) would like to thank the Carilion Biomedical Institute for financial support.

¹G. M. Whitesides, J. P. Mathias, and C. T. Seto, *Science* **254**, 1312 (1991).

²See, for example, a review, Y. Xia, J. A. Rogers, K. E. Paul, and G. M. Whitesides, *Chem. Rev.* **99**, 1823 (1999).

³In this letter, a block copolymer monolayer is defined as a thin film with thickness such that the discrete phase forms a monolayer, E. L. Thomas, D. J. Kinning, D. B. Alward, and C. S. Henke, *Macromolecules* **20**, 2934 (1987); P. Mansky, P. Chaikin, and E. L. Thomas, *J. Mater. Sci.* **30**, 1987 (1995); *Appl. Phys. Lett.* **68**, 2586 (1996).

⁴See, for example, a review, F. S. Bates and G. H. Fredrickson, *Phys. Today* **52**, 32 (1999).

⁵M. Park, C. Harrison, P. M. Chaikin, R. A. Register, and D. H. Adamson, *Science* **276**, 1401 (1997), and references therein.

⁶C. Harrison, M. Park, P. M. Chaikin, R. A. Register, and D. H. Adamson, *J. Vac. Sci. Technol. B* **16**, 544 (1998).

⁷C. T. Black, K. W. Guarini, K. R. Milkove, S. M. Baker, T. P. Russell, and M. T. Tuominen, *Appl. Phys. Lett.* **79**, 409 (2001).

⁸T. Thurn-Albrecht, R. Steiner, J. DeRouchey, C. M. Stafford, E. Huang, M. Bal, M. Tuominen, C. J. Hawker, and T. P. Russell, *Adv. Mater.* **12**, 787 (2000).

⁹T. L. Morkved, M. Lu, A. M. Urbas, E. E. Ehrichs, H. M. Jaeger, P. Mansky, and T. P. Russell, *Science* **273**, 931 (1996); T. Thurn-Albrecht, J. DeRouchey, T. P. Russell, and H. M. Jaeger, *Macromolecules* **33**, 3250 (2000).

¹⁰C. C. Honeker, E. L. Thomas, R. J. Albalak, D. A. Hajduk, S. M. Gruner, and M. C. Capel, *Macromolecules* **33**, 9395 (2000).

¹¹C. DeRosa, C. Park, E. L. Thomas, and B. Lotz, *Nature (London)* **405**, 433 (2000).

¹²P. Mansky, Y. Liu, E. Huang, T. P. Russell, and C. Hawker, *Science* **275**, 1458 (1997).

¹³R. R. Li, P. D. Dapkus, M. E. Thompson, W. G. Jeong, C. Harrison, P. M. Chaikin, R. A. Register, and D. H. Adamson, *Appl. Phys. Lett.* **76**, 1689 (2000).

¹⁴T. Thurn-Albrecht, J. Schotter, C. A. Kastle, N. Emley, T. Shibauchi, L. Krusin-Elbaum, K. Guarini, C. T. Black, M. T. Tuominen, and T. P. Russell, *Science* **290**, 2126 (2000).

¹⁵Y. Lee, N. Yao, and I. A. Aksay, *Langmuir* **13**, 3866 (1997).

¹⁶L. D. Landau and E. M. Lifschitz, *Electrodynamics of Continuous Media*, 2nd ed. (Oxford University Press, New York, 1984).

¹⁷K. Amundson, E. Helfand, X. Quan, and S. D. Smith, *Macromolecules* **26**, 2698 (1993).

¹⁸T. Thurn-Albrecht, J. DeRouchey, T. P. Russell, and H. M. Jaeger, *Macromolecules* **33**, 3250 (2000).

¹⁹S. Niu, E. Stumb, and R. F. Saraf, *Appl. Phys. Lett.* **80**, 4425 (2002).

²⁰H. Liew, R. B. Meyer, and A. J. Hurd, *J. Appl. Phys.* **55**, 2809 (1984).

²¹A. Budkowski, J. Klein, and L. W. Fetters, *Macromolecules* **28**, 8571 (1995).

²²R. A. Segalman, H. Yokoyama, and E. J. Kramer, *Adv. Mater.* **13**, 1152 (2001).